Partial Atomic and Ionic Stopping Powers of Gaseous Hydrogen for Helium and Hydrogen Beams*

J. CUEVAS, M. GARCIA-MUNOZ, P. TORRES,† AND S. K. ALLISON
The Enrico Fermi Institute for Nuclear Studies, The University of Chicago, Chicago, Illinois
(Received 24 February 1964)

The partial stopping power of a target material for an ion or an atom is the energy lost per target particle per cm² in all types of collisions in which the ion or the atom is the projectile, with the exception of those collisions in which the projectile leaves with its charge changed. Partial atomic stopping powers of target gases for atoms are measured by imposing a strong transverse magnetic field on the stopping cell. For partial ionic stopping-power measurements, the ion beam is held in a circular orbit, closely defined by vanes and slits, as it traverses the stopping cell. The partial stopping powers ϵ_0 (for He^0 traversing H_2 gas), ϵ_1 (for He^+), ϵ_2 (for He^{++}) have been measured in the kinetic energy range 40–460 keV, and new measurements of the ordinary, or total stopping power of H_2 gas for helium from 40 to 220 keV have been made. Using the known charge composition of He beams in H_2, it is possible to deduce the fraction of the stopping power losses due to charge changing collisions, and this varies from 37% at 140 keV to 27% at 400 keV. At 120 keV, the total energy loss in completing the charge changing cycle $He^+ \rightarrow He^0 \rightarrow He^+$ is 95±9 eV, rising to 117±10 at 160 keV.

INTRODUCTION

HELIUM ions and atoms in the kinetic energy range 30–480 keV have velocities lying in the range 1.2 to 4.8×10^8 cm/sec or 0.55 to 2.2 in units of $e^2/\hbar$. Capture and loss of electrons by these projectiles are prominent types of inelastic collisions, and a helium beam traversing matter rapidly comes to a charge equilibrium characteristic of the medium and the velocity. We shall represent the equilibrium fractions of He^0, He^+, and He^{++} present in H_2 gas by $F_{0\infty}$, $F_{1\infty}$, and $F_{2\infty}$, respectively, and Fig. 1 shows the collected results of several studies of such $F_{i\infty}$ values.[1–4] In the energy range 30–175 keV, we see that at equilibrium we have essentially a two-component system composed of He^0 and He^+, since here $F_{2\infty}<0.010$. In the region 175–450 keV, we must treat the equilibrated beam as a three-component system.

In order to obtain a sufficient energy decrement $-\Delta E$ for accuracy in a standard stopping-power measurement, much more material is customarily placed in the beam than is necessary to produce charge equilibrium. Each projectile completes an electron capture and loss cycle many times in traversing the absorber,[5] and the observed total loss is a weighted mean of the losses in many types of inelastic collisions. Those usually considered in stopping theory are excitation and ionization of the target medium; in our case there are, in addition, the energy losses in electron capture, and, during the period when the projectile is a moving atom or an incompletely stripped ion, losses in excitation and ionization of the projectile.

Recently,[6,7] an experimental technique has been introduced which allows an analysis of the total stopping power into several contributions. These are called partial stopping powers, and are the specific energy losses for projectiles which, in their traversal of the absorber, never change their charge state. The contribution from inelastic collisions in which the projectile captures or

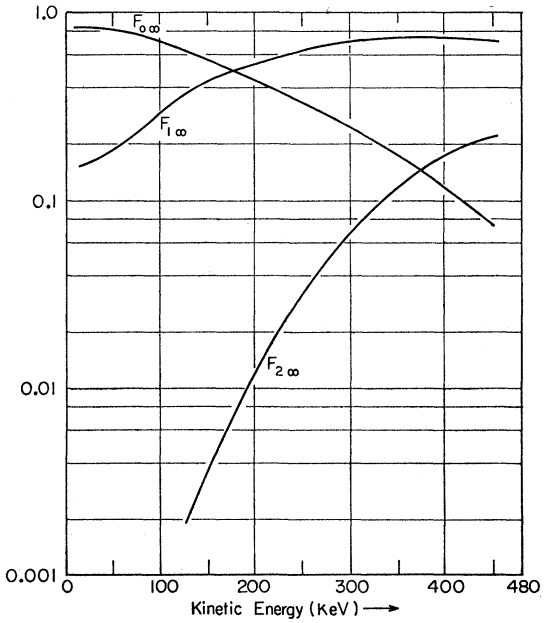

FIG. 1. The equilibrium charge composition of a helium beam traversing gaseous hydrogen.

* This work was supported in part by the U. S. Atomic Energy Commission.

† Fellow of the Argentine National Research Council and Centro Atómico Bariloche, Argentine.

[1] E. Snitzer, Phys. Rev. **89**, 1237 (1953).

[2] C. F. Barnett and P. M. Stier, Phys. Rev. **109**, 385 (1958).

[3] S. K. Allison, Phys. Rev. **109**, 76 (1958).

[4] S. K. Allison, Rev. Mod. Phys. **30**, 1137 (1958).

[5] In a simple capture and loss cycle involving He^0 and He^+ in a beam of kinetic energy E electron volts, the number of cycles completed in an absorber is easily shown to be $\sigma_c|\Delta E|/\epsilon$ where $|\Delta E|$ is the magnitude of the energy decrement in eV, ϵ is the standard or total stopping power, and $\sigma_c=\sigma_{01}\sigma_{10}/(\sigma_{01}+\sigma_{10})$ is the cross section for cycle completion [cf. Ref. 4, Eq. (III-3)]. In the lower energy range specified above, if $|\Delta E|/E\sim0.1$, the number varies from 20 to 50.

[6] S. K. Allison, J. Cuevas, and M. Garcia-Munoz, Phys. Rev. **127**, 792 (1962).

[7] M. N. Huberman, Phys. Rev. **127**, 799 (1962).

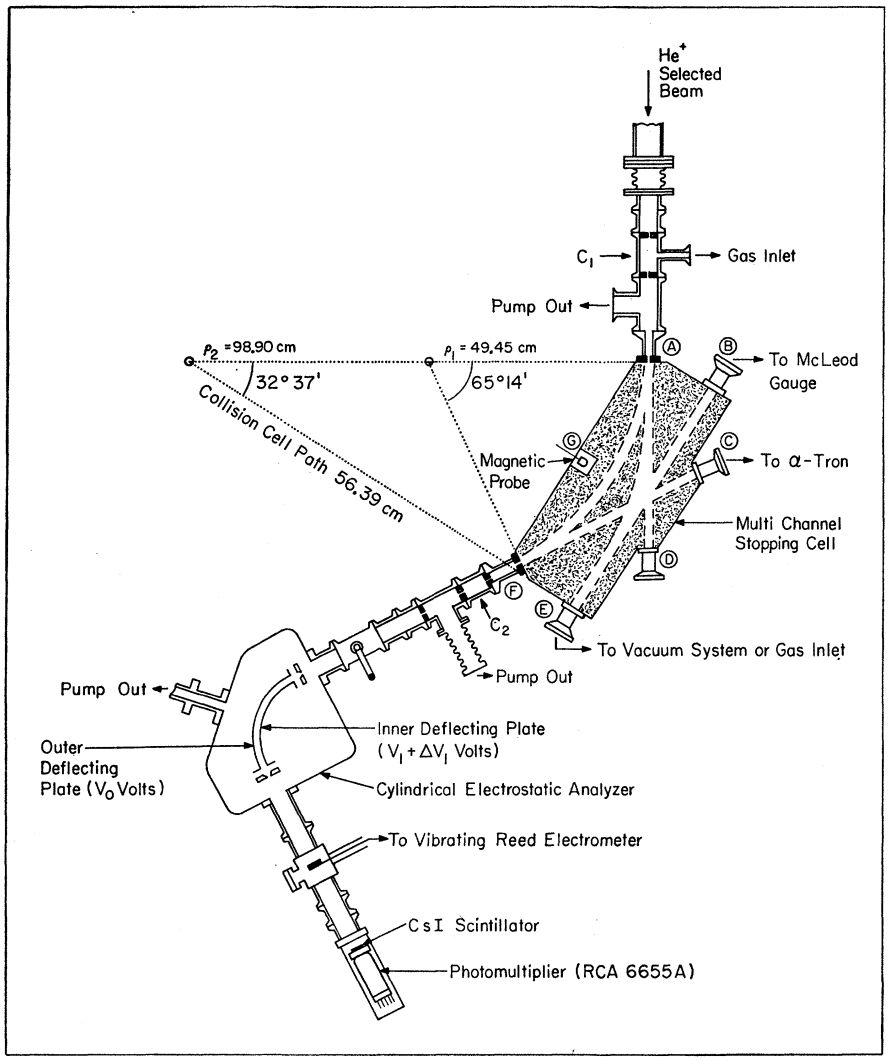

FIG. 2. Apparatus for measuring atomic and ionic partial stopping powers shown arranged for the measurement of ϵ_1 or ϵ_2. For the measurement of ϵ_0 the system is rearranged so that the beam enters the stopping cell at B and leaves it at E. The openings C and D are for alignment purposes.

loses electrons is obtained as the difference between the total stopping power and the weighted sum of the partial stopping powers.

The method of measurement of partial atomic and ionic stopping powers has been extensively discussed[6,7] so that only a brief outline is given here. The ion accelerator, with its sorting magnet, produces a beam of He^+ ions. If a measurement of a partial stopping power other than that for He^+ (i.e., other than ϵ_1) is desired, the beam is first brought to charge equilibrium in cell C_1 of Fig. 2. For a measurement of ϵ_2, the magnetic field in which the stopping cell is placed is adjusted so that He^{++} follows the channel from A to F, and eventually enters the electrostatic analyzer where its energy is measured. The partial stopping power ϵ_2 is then determined by admitting the stopping gas (H_2) to channel AF. The experiment operates on a narrow margin of feasibility, but it is possible to admit enough gas to produce a measurable energy decrement without diminishing the beam intensity, through losses due to electron capture, below a value at which good statistics may be obtained by counting single particles. For ϵ_1, where the component to be measured is the same as that produced by the beam accelerator, the procedure is similar to that for ϵ_2, but it is not necessary to equilibrate the beam in C_1, and the magnetic field must be set so that He^+ follows the path from A to F.

If ϵ_0 is to be measured, the entrance and exit trains of equipment are disconnected from the stopping cell at A and F, respectively, and reattached at B and E, so that BE is a "straight through" channel. The magnetic field is set at a high value so that only particles remaining neutral from B to E enter C_2. In order to analyze these neutrals electrostatically, some of them are stripped to He^+ by admitting a few microns of gas to cell C_2. Small amounts of gas, measurable in microns, are admitted to the channels of the stopping cell and the energy losses due to collisions in which there is no

change of charge are measured, as before,[6,7] by noting ΔV_1.

The ordinary or total stopping power ϵ may be measured with the apparatus arranged as for ϵ_0, but with the magnetic field off. It is not necessary to have gas in C_1 or C_2 for such a determination, but (as is also true for ϵ_i measurements) the presence of gas in C_1 or C_2 does not affect the energy decrement of interest, due to pressure changes in the stopping cell.

The ordinary or total atomic stopping power ϵ of the medium for the projectile beam is defined as

$$\epsilon=-(1/N)(dE/dx) \quad \text{eVcm}^2/\text{atom}. \tag{1}$$

dE/dx is the energy change (a loss) in eV per cm of path in the medium. N is the number of atoms per cubic centimeter in the medium.

If, as is true in the usual total stopping-power determination, the energy change ΔE produced for measurement is so large that it includes the contributions from all the various possible types of inelastic collisions, but at the same time is so small that the change of ϵ in the energy range E–ΔE may be neglected, we may write

$$\epsilon=-\frac{1}{N}\frac{\Delta E}{\Delta x}=\sum_i F_{i\infty}\epsilon_i+\sum_{i,f} F_{i\infty}\sigma_{if}W_{if}. \tag{2}$$

$F_{i\infty}\epsilon_i$ represents the part of the total energy loss attributable to ions of charge $i|e|$, or atoms ($i=0$), due to their inelastic impacts in which no change of the projectile's charge is involved. W_{if} is the energy loss in eV in an inelastic collision in which the projectile's charge changes from i to f. σ_{if} is the cross section in cm² per atom of target gas for a collision in which the projectile's charge is changed from i to f. In greater detail, W_{if} is in itself a weighted sum, since a collision in which the projectile's charge changes from i to f may leave the target atom in various states, corresponding to the transfer of various amounts of energy.

The experimental results reported here are measurements of the partial stopping powers ϵ_0, ϵ_1, and ϵ_2, in the kinetic energy range 30–480 keV, and of ϵ in the previously unexplored region 40–150 keV for a helium beam in hydrogen gas.

APPARATUS AND EXPERIMENTAL PROCEDURE

The basic equipment, and the experimental technique for partial stopping power measurements have been discussed in considerable detail.[6,7] The present work on helium beams was begun using the same equipment described by Huberman[7] in his work with hydrogen beams. We only mention here several improvements which were developed in the course of the helium work.

A. The Stopping Cell

The most significant change was the installation of a new multichannel stopping cell, the need for which became apparent in our attempts to measure ϵ_1 for He^+.

With the He^+ beam held in orbit, so that the charge changes $He^+ \rightarrow He^0$ or $He^+ \rightarrow He^{++}$ remove the particle from the beam the most important factor by which the intensity is diminished as gas is admitted is $\exp[\Delta E(\sigma_{10}+\sigma_{12})/\epsilon_1]$ where ΔE is the change in transmitted beam energy in eV produced on admission of gas, ϵ_1 is the ionic partial stopping power, and σ_{10}, σ_{12} are the appropriate charge-changing cross sections. ΔE depends on the amount of gas admitted; the minimum ΔE for which a sufficiently accurate measurement is possible should be about the energy spread at half-maximum of the beam supplied by the accelerator.[8] At 150 keV, our energy spread was 0.65%; we used $\Delta E\sim-1.78$ keV. $(\sigma_{10}+\sigma_{12})=7.3\times10^{-17}$ cm², and $\epsilon_1=6.1\times10^{-15}$ eV×cm²/atom. Thus the loss in intensity corresponds to a factor of $10^{-9.2}$. The factor for the measurement of ϵ_1 for protons in H_2 gas at 55 keV, is $10^{-7.5}$, calculated from $\Delta E=-1.06$ keV, $\epsilon_1=5.4\times10^{-15}$, and $\sigma_{10}=8.8\times10^{-17}$. Thus at these energy spreads, the helium determination at 150 keV is considerably the more difficult, since about 50 times more particles are removed from the beam and contribute to the background of scattered particles. Since $\sigma_{10}/\sigma_{12}=30$, most of these accumulate in the angular region between the direct beam and the exit aperture for He^+, and for Huberman's stopping cell this deviation was only 21°. Also there were no internal vanes or stops in the stopping cell to limit the effective scattering volume, and in spite of the 0.05 cm slit in front of the electrostatic analyzer it was unfortunately easy to flood the analyzer with this huge background and measure a spurious stopping power due to scattered particles. Our first results on ϵ_1 using Huberman's cell fluctuated widely and were unreliable.

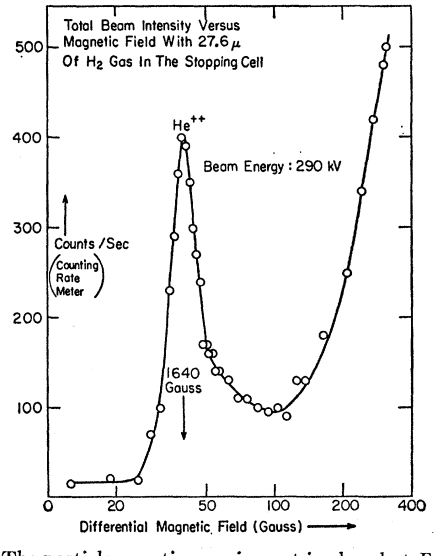

FIG. 3. The particle-counting equipment is placed at F (Fig. 2), and, with gas in, the intensity of the emergent beam is recorded as a function of magnetic field strength.

[8] See Fig. 3, Ref. 7.

Two obvious improvements are to increase the angle of deviation of the He^+ beam, and to reduce the volume of gas from which scattering can reach the exit aperture. These improvements were incorporated into a new stopping cell (Fig. 2), in which two angular deviations (32°37′ and 65°14′) were possible, and the orbits centered in tubular channels 1.2 cm in diameter in an otherwise solid brass block. Before measuring a partial ionic stopping power, a curve such as Fig. 3 was always taken by replacing the electrostatic analyzer by the scintillation counter (Fig. 2) and measuring counts per second as a function of the magnetic field in the stopping cell. The pressure in the cell was raised to a value equal to or slightly above that which would ultimately be used for the ϵ_i measurement. Thus it was established that although the orbital beam was greatly reduced in intensity, it nevertheless stood out well above the background. For the ϵ_i measurement itself the equipment was put back into the disposition of Fig. 2 and the magnetic field with gas in reduced very slightly so that the beam entering the electrostatic analyzer was the peak of a curve such as that of Fig. 3. With these precautions the fluctuations in the measurements largely disappeared.

B. Types of Ion Sources

With the radio-frequency ion source[9] used in the first part of the present work the energy shape of the beam, as measured with no gas in the stopping cell, showed a double-peaked structure[10] which is believed to be due mostly to the energy distribution of the ions as they originate in various parts of the cathode fall region of the source. The reference point for associating an energy value to each peak distribution was taken as midway between the steepest slopes of the leading and end edges. The two structure peaks were about the same height in most of the measurements so that the edge symmetry was not noticeably affected by their presence. But in some measurements uncontrollable changes in the ion source made one of the structure peaks much smaller than the other, introducing an uncertainty in locating the reference point.

In an attempt to avoid the double-peaked energy profile we investigated the energy profile from a low-voltage-arc ion source.[11] The usual reason for discarding such sources is that, with hydrogen, most of the emission is in the form of molecular ions rather than protons; this objection does not hold for helium. The entire voltage drop along the arc canal is about 30 V and the ions used are all formed in a region where the potential cannot vary more than a small fraction of this amount. The beam from this arc when accelerated and analyzed into an energy-versus-intensity profile had widths about 20% less than from the radio-frequency source and, what was more important, the double-peaked structure disappeared leaving a simple maximum. Therefore the readings (below 350 keV, for other technical reasons) were mostly carried out with the older type of source.

The assurance that the energy-intensity profiles would have only one maximum made it possible to make determinations much more rapidly than before, since only the peaks of the "gas in" and "gas out" profiles had to be located, whereas previously the entire shape had to be explored.

With 0.1-cm-slit width at entrance and exit of the electrostatic analyzer the energy width at half-maximum of the beam was approximately 1.3% at 50 keV, 0.6% at 120 keV, and 0.5% at 200 keV.

C. Beam and Particle Detecting Equipment

The Allen-type electron-multiplier tube detector previously used[12] was eventually discarded. Although it proved rugged and easy to operate it had two limitations in extracting the maximum possibilities from the experiment: first, small electric leaks in the dynode connections caused a rather high level of noise and second, the multiplier gain decreased slowly but steadily with time so that after a few weeks' operation it had to be taken out of the system and subjected to a dynode baking process. To improve the individual particle counting the electron multiplier tube was replaced by a scintillation counter built up of a CsI crystal and a RCA 6655-A photomultiplier tube. The crystal was 13 mm in diameter and 0.3 mm thick in order to keep the scintillation background very low. This new counter proved to be durable, with very low total background and increased the counting efficiency by about 50%. This counter was not, of course, suitable to the measurement of the high intensity of the "gas out" beams. In this case the beam was intercepted on a brass vane (cf. Fig. 2) and the current measured on a vibrating reed electrometer.

D. Accelerator High-Voltage Control

Although the determination of stopping power is primarily a measurement of change in energy, fluctuations in intensity during the measurement can reduce the accuracy of the measurement. Actually energy and intensity at the final detector are closely related since a shift in the energy of the beam from the accelerator, small in comparison to the energy losses due to stopping power, greatly decreased the intensity because of the resultant differences in the magnetic and electric deviations and the large number of narrow apertures. As an interim substitute for a fully automatic feed-back energy control (now under consideration) the primary of the accelerator transformer was provided with a manually operated fine adjustment circuit by which the volt-

[9] E. Norbeck and S. K. Allison, Rev. Sci. Instr. **27**, 285 (1956).
[10] See Fig. 3 of Ref. 6, also Fig. 3 of Ref. 7.
[11] S. K. Allison, Rev. Sci. Instr. **19**, 291 (1948).
[12] See Ref. 6 and J. S. Allen, Phys. Rev. **55**, 336 (1939).

TABLE I. Remeasurements of ϵ_1 for hydrogen beams in H_2 gas. ϵ_1 in units of 10^{-15} eV×cm²/atom.

Previous determinations		New determinations	
Kinetic energy (keV)	ϵ_1	Kinetic energy (keV)	ϵ_1
44.8	6.12±0.44	40.5	5.29±0.5
		40.7	5.45±0.3
		52.3	5.32±0.4
55.0	5.70±0.6	52.4	5.60±0.6
56.7	6.04±0.39	53.3	4.90±0.4
		53.4	5.57±0.2
75	5.70±0.6		
93	5.07±0.5		

age could be kept in a range about 100 eV wide as determined by the galvanometer of the high-voltage monitoring system. Further intensity adjustments were made by varying the charge on the beam shifting electrostatic deflector plate installed in the accelerator, and by minute changes in the magnetic deflections. The beam-energy mean values thus obtained showed standard deviations of about ±3 V.

III. RESULTS

A. Remeasurement of ϵ_1 for H^+ in H_2 Gas

Following the installation of the new stopping cell and the procedure of making sure, through curves similar to Fig. 3, that an energy degraded ionic H^+ beam remained well above the background we repeated the measurements of Huberman[7] on ϵ_1 for H^+. Deuterons of energies $2E$ were used to simulate protons of energy E in these experiments, since many previous runs have shown no differences in their behavior at the same velocity, and our accelerator focused better at higher energies. The results are shown in Table I.

TABLE II. Typical determinations of partial and total stopping powers.

Experimental conditions	Quantity being measured ϵ_0	ϵ_1	ϵ_2	ϵ
Beam energy (keV)	328	333	342	328
Pressure of H_2 admitted to stopping cell (microns)	33.5	43.7	29.8	33.5
Length of beam path in stopping cell (cm)	58.5	56.39	56.39	58.5
Length of beam path in compartment adj. to stopping cell (cm)	48	39	39	48
Pressure in outer compartments (microns)	0.14	0.65	0.41	0.14
Energy change in beam (keV)	−0.816	−1.445	−0.819	−1.590
Partial or total stopping power eV×cm²/atom	6.43×10^{-15}	8.98×10^{-15}	14.5×10^{-15}	12.5×10^{-15}
Magnetic field on stopping cell (gauss)	3060	3450	1720	···

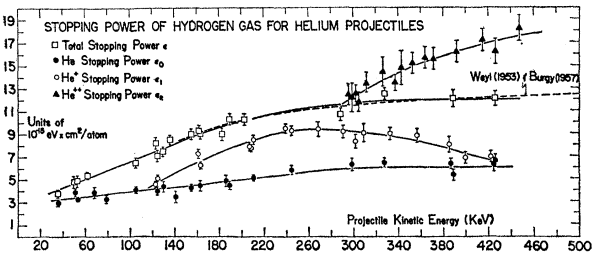

FIG. 4. Experimental atomic and ionic partial stopping powers for He^0, He^+, and He^{++} traversing molecular hydrogen gas.

The largest discrepancy between our new and the old results is near 40 keV where the average of the new measurements at 40.5 and 40.7 keV is 12% lower than Huberman's ϵ_1 value at 44.8 keV. We consider the new values to be preferable.

It is consistent with our interpretation of the errors to be avoided by the construction of the new stopping cell that the new ϵ_1 values are slightly lower, not higher, than the previous ones. The larger admixture of scattered particles in the older measurements would introduce beam constituents which had traveled a greater distance in the old stopping cell than the true orbital path, and had thus experienced charge-changing collisions both of which increase the energy loss beyond that truly attributable to ϵ_1.

B. Results on Helium Beams

Data taken in typical measurements of partial stopping powers of hydrogen gas for helium beams is given in Table II, and from it an idea of the actual experimental conditions may be obtained. The collected re-

TABLE III. Total and partial stopping powers for helium beams traversing hydrogen gas.

Kinetic energy (keV)	ϵ's measured in units of 10^{-15} eV×cm²/atom ϵ (a)	ϵ (b) Weyl	ϵ_0	ϵ_1	ϵ_2
40	4.3±0.4		3.3±0.4		
60	5.1		3.5		
80	5.8		3.8		
100	6.6		4.0		
120	7.3		4.2	4.8±0.3	
140	8.1		4.4	5.5	
160	8.9	9.1±0.4	4.6	6.5	
180	9.6	9.6	4.8	7.3	
200	10.2	10.2	5.0	8.1	
220	10.5±1.0	10.5	5.2±0.6	8.7±0.4	
250	11.2	11.0	5.6	9.3	
275	11.5	11.2	5.8	9.4	
300	11.7	11.5	6.0	9.2	12.2±1.1
325	11.8	11.7	6.0	8.8	13.6
350	12.0	11.9	6.0	8.5	14.8
375	12.0	12.0	6.0	7.9	15.7
400	12.0	12.1	6.0	7.3	16.4
425	12.0	12.2	6.0	6.5±0.4	17.0
450	12.0	12.3	6.0±0.7	···	17.6±1.0

[a] Measured with same equipment as for partial stopping powers ϵ_0.
[b] P. K. Weyl, Phys. Rev. 91, 239 (1953).

sults are shown in the graphs of Fig. 4 and numerical values based on smooth curves drawn through the experimental points are shown in Table III.

IV. DISCUSSION OF RESULTS

A. Analysis of Processes Comprised in Partial Stopping Powers and in Charge-Changing Collisions

Table IV shows some of the possible modes of interaction of a helium particle and a moleule of hydrogen gas in a collision in which there is sufficient energy available to dissociate both partners completely into a helium nucleus, protons, and electrons. Modes which are possible, but considered to be of negligible importance for these experiments, such as the excitation of vibrational states in H_2^+ and H_2 and the formation, by capture, of He^- or H_2^- are not listed. Also "fine structure" effects such as spin orientations, are not considered. It is seen that, even with the experimental partition of the stopping process, each partial stopping power represents many possible modes of inelastic collision.

B. The Fraction of the Energy Loss Due to Collisions in Which the Projectile's Charge is Changed

If we expand the sum of the weighted partial stopping powers in Eq. (2) in a form suitable to helium beams in hydrogen, and neglect[13] He^-, we obtain

$$\epsilon = F_{0\infty}\epsilon_0 + F_{1\infty}\epsilon_1 + F_{2\infty}\epsilon_2 + \sum_{if} F_{i\infty} W_{if}\sigma_{if}. \qquad (3)$$

Since in certain energy regions we have measured ϵ_0, ϵ_1, ϵ_2, and ϵ, and the F's are known (Fig. 1), we can obtain the energy losses per atom per cm² due to collisions in which the charge of the projectile is changed. The result is shown, as fractions of the total stopping power ϵ, in Fig. 5.

The measurements establish the fraction of the energy loss due to charge-changing collisions in the kinetic energy regions 140–180 and 300–420 keV. We have extrapolated the curve from 140 down to 80 keV and established limits at 40 keV with some assurance in consideration of the following facts and assumptions. We have measured $F_{0\infty}\epsilon_0/\epsilon$ in this 80–140-keV region. Physical expectation and the data of Tables II and III show that ϵ_1 for He^+ should be roughly the same as for H^+ at these relatively low velocities (1.10 to 1.25 in $e^2/\hbar$ units), and hence lie in the range 3–5 in units of

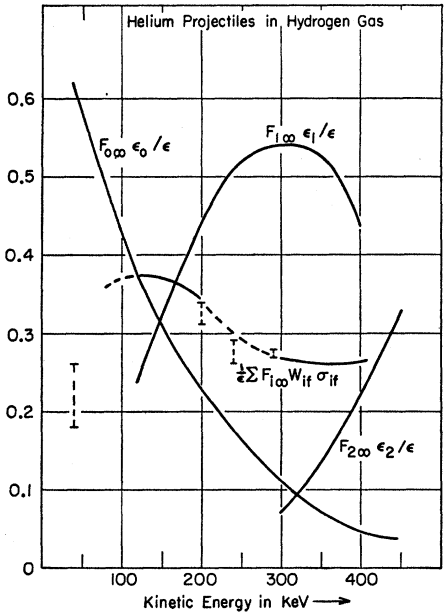

FIG. 5. The fraction of the total stopping power attributable to He^0, excepting electron-loss collisions; to He^+, excepting capture or loss; and to He^{++} excepting capture. $[\Sigma F_{i\infty}W_{if}\sigma_{if}]/\epsilon$ is the fractional loss in collisions involving change of charge of the projectile.

TABLE IV. Summary of possible reaction products following a $He-H_2$ collision (disregarding the formation of negative ions by electron capture).

I. Final products from H_2 following an inelastic collision with no charge change of the projectile:
1. H_2(exc)
2. H+H
3. H(exc)+H
4. H(exc)+H(exc)
5. $H^+ + H^-$
6. $H_2^+ + e$
7. H_2^+(exc)$+e$
8. $H + H^+ + e$
9. H(exc)$+H^+ + e$
10. $H^+ + H^+ + 2e$

II. Final hydrogenic and electronic products following an inelastic collision with the capture of one electron by the projectile:
1. H_2^+
2. H_2^+(exc)
3. $H + H^+$
4. H(exc)$+H^+$
5. $H^+ + H^+ + e$

III. Final hydrogenic and electronic products following an inelastic collision with the capture of two electrons by the projectile:
1. $H^+ + H^+$

IV. Reactions allocated to ϵ_0 for He^0:
(a) $He^0 + H_2 \rightarrow He^0 + I(1\text{–}10)$
(b) $He^0 + H_2 \rightarrow He^0(\text{exc}) + I(1\text{–}10)$

V. Reactions allocated to ϵ_1 for He^+:
(a) $He^+ + H_2 \rightarrow He^+ + I(1\text{–}10)$
(b) $He^+ + H_2 \rightarrow He^+(\text{exc}) + I(1\text{–}10)$

VI. Reactions allocated to ϵ_2 for He^{++}:
(a) $He^{++} + H_2 \rightarrow He^{++} + I(1\text{–}10)$

VII. Reactions[a] allocated to $\Sigma F_{i\infty}W_{if}\sigma_{if}$:
(a) $He^0 + H_2 \rightarrow He^+ + e + I(1\text{–}10)$,[a]
(b) $He^0 + H_2 \rightarrow He^{++} + 2e + I(1\text{–}10)$,
(c) $He^+ + H_2 \rightarrow He^0 + II(1\text{–}5)$,[a]
(d) $He^+ + H_2 \rightarrow He^{++} + e + I(1\text{–}10)$
(e) $He^{++} + H_2 \rightarrow He^+ + II(1\text{–}5)$,[a]
(f) $He^{++} + H_2 \rightarrow He^0 + 2H^+$

[a] Plus reactions leaving the He atom or ion in excited states.

[13] T. Jorgensen Jr., Proc. Gatlinburg Conf., Natl. Acad. Sci.–Natl. Research Council Publ. No. 752, p. 72 (1960).

TABLE V. Sum of the energy decrements in the electron capture and subsequent loss cycle for H^+ and He^+ ions in hydrogen gas.

Hydrogen projectiles[a]		Helium projectiles	
Kinetic energy (keV)	$(W_{01}+W_{10})$ (eV)	Kinetic energy (keV)	$(W_{01}+W_{10})$ (eV)
43	45±6	120	95±9
54	63±9	140	103±10
75	107±22	160	117±10
93	147±29	···	···

[a] M. N. Huberman, Ref. 6; his original values slightly increased to conform to Table I.

10^{-15} eV×cm²/atom. Using values of the F's from Fig. 1 we see that the fractional contribution from the charge-changing term probably lies between 0.17 and 0.26 at 40-keV He^+ kinetic energy, as indicated in Fig. 5. Thus, the fractional contribution from charge changing for a He beam must have a maximum near 0.37 between 40 and 150 keV.

The interpolation between 180 and 300 keV is based on various methods of extrapolating the curve $F_{2\infty}\epsilon_2/\epsilon$ to zero below 300 keV. The range in which the charge changing fractional contribution must lie is not very sensitive to different possible extrapolations. It seems reasonable to expect that there will be a second maximum in the fractional charge-changing contribution in the neighborhood of 600 keV, where the cycle cross section $\sigma_{12}\sigma_{21}/(\sigma_{12}+\sigma_{21})$ has a maximum.

C. Energy Expended in the Charge-Changing Cycle $He^0 \rightleftarrows He^+$

The expansion of the charge-changing sum involved in Eq. (3), for the case of helium is

$$\sum_{if} F_{i\infty}W_{if}\sigma_{if}=F_{0\infty}(W_{01}\sigma_{01}+W_{02}\sigma_{02}) +F_{1\infty}(W_{10}\sigma_{10}+W_{12}\sigma_{12}) +F_{2\infty}(W_{20}\sigma_{20}+W_{21}\sigma_{21}). \quad (4)$$

In the kinetic energy region 120–160 keV, the σ's and F's are all known.[4] The value of $F_{2\infty}$ does not exceed 0.006, and the values of σ_{12}/σ_{10} and σ_{02}/σ_{01} are $\leqq 0.04$. Hence, in this region, until the accuracy of measurement of partial stopping powers is considerably improved, the significant terms of Eq. (4) are

$$\sum_{if} F_{i\infty}W_{if}\sigma_{if}\doteq F_{0\infty}W_{01}\sigma_{01}+F_{1\infty}W_{10}\sigma_{10} \doteq[\sigma_{01}\sigma_{10}/(\sigma_{01}+\sigma_{10})][W_{01}+W_{10}]. \quad (5)$$

Thus we can deduce, from our measurements, the sum of the energies lost in the inelastic collisions which initiate and terminate a charge-changing cycle. These are collected and compared with the analogous result of Huberman for hydrogen beams in hydrogen gas in Table V.

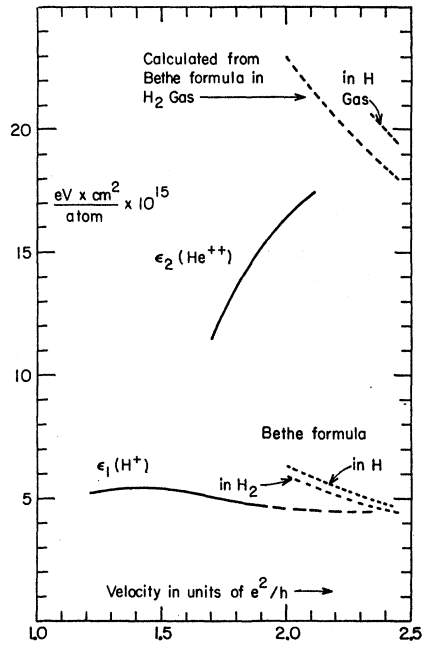

FIG. 6. Experimental partial stopping powers of H_2 gas for protons and for alpha particles. Dashed curves are calculated values using Bethe's equation (Table VII) with 1.105 $Rh\equiv I=15$ for H gas and $I=19$ for H_2 gas.

D. Partial Stopping Power for Protons and Helium Nuclei

Figure 6 shows the partial stopping powers of hydrogen gas for protons and for helium nuclei. The inelastic collisions contributing to the energy losses concerned may be considered as those initiated by moving point charges of $Z=1$ and $Z=2$, respectively, with the exclusion of those events resulting in electron capture. The ϵ_1 curve for protons has been extrapolated beyond the highest energy measured (93 keV; $v=1.93\ e^2/\hbar$) up to 140 keV where $v=2.37\ e^2/\hbar$. This can be done from Eq. (2). The values of i are limited to 0 and 1; $F_{0\infty}$, ϵ_0, and ϵ are known from experiment, and the charge-changing term, which contributes very little, can be estimated with sufficient accuracy by extrapolating $(W_{01}+W_{10})$ values from Table V and using the known values of σ_{01} and σ_{10}.

Bethe's well-known theoretical treatment of the stopping of protons and alpha particles uses the Born approximation, and does not include losses due to electron capture. It leads to the well-known formulas given in the upper part of Table VII, and thus their validity is limited to regions of high velocity ($\gg e^2/\hbar$ for H^+ and $\gg 2e^2/\hbar$ for He^{++}). For projectiles of lower and lower velocities, the experimental values of the total stopping power ϵ may be expected to deviate from such theoretical calculations because of failure of the Born approximation and neglect of the velocities of the electrons in the target atom, and of the initiation and increasing prominence of electron captures and losses which change

TABLE VI. Energies lost by protons in H_2 gas due to ionization and to excitation and dissociation.

E (keV)	$Q(e)$ (cm²/mole)	$W(e)$ (eV)	$Q(e)W(e)$ eV×cm²/mole	$2\epsilon_1$	$Q^*(d)W^*(d)/2\epsilon_1$ exp	DG(1955)
50	26×10^{-17}[a]	38.0[e]	9.9	11.0[e]	0.10	0.26[f]
100	21.3×10^{-17}[b]	43.8[d]	9.32	10[e]	0.07	0.25[f]

[a] Schwirzke's value, used by KJ.
[b] Absolute determination by RJ.
[c] KJ (Ref. 17).
[d] RJ (Ref. 18).
[e] Table I, this paper.
[f] Calculated by Dalgarno and Griffing (Ref. 18) for atomic hydrogen targets.

the projectile's charge. Since the latter two events are excluded in the experimentally measured partial stopping powers $\epsilon_1(H^+)$ and $\epsilon_2(He^{++})$, a study of their deviations from Bethe's equation at such low velocities is more meaningful in detecting breakdown of the fundamental theoretical assumptions than is a comparison of the theory with the observed total stopping powers.

Calculations of the stopping power of atomic hydrogen gas ($I=15$ eV) and of molecular hydrogen gas ($I=19$ eV) are given in columns 4,5, and 9,10 of Table VIII, and plotted with the partial stopping powers in Fig. 6. It is clear that the partial stopping power of H_2 gas for protons will asymptotically coincide with the Bethe calculation at about 140 keV. At lower energies, the Bethe formula overestimates the partial stopping power. Dalgarno[14] has remarked that the Bethe theory overestimates the total stopping power in this region; his statement is seen to be also true of the partial stopping power.

In Fig. 6 it is also shown that the Bethe formula overestimates the partial stopping power $\epsilon_2(He^{++})$ although ϵ_2 is here greater than the total ϵ. $\epsilon_2(He^{++})$ is apparently attaining the values calculated from the Bethe formula at about 2.4 $e^2/\hbar$, as does the partial stopping power for protons, but the experiments have not been extended sufficiently to demonstrate the type of approach to the theoretical curves. It may be noted that the ratio $\epsilon_2(He^{++})/\epsilon_1(H^+)$ is apparently rising with velocity toward the theoretical value of 4. It has attained 3.7 at 2.22 $e^2/\hbar$; the ratio of the total stopping powers does not attain this value until the velocity has reached 3.3 $e^2/\hbar$, showing the simpler nature of the partial stopping-power ratio.[15]

E. Evidence Concerning the Relative Losses of Proton Projectiles in Excitation and in Ionization of H_2 Gas

From items VI and I of Table IV, but applied to protons as projectiles rather than to alpha particles, we see that the reactions contributing to $\epsilon_1(H^+)$ can be classified as producing free electrons (I-6 to I-10), or as resulting in excitation or dissociation of the H_2 target (I-1 to I-5). If the total cross section per molecule of H_2 for the former is $Q(e)$ and of the latter is $Q^*(d)$, and if $W(e)$ and $W^*(d)$ are the energies lost by the projectile per event, then

$$2\epsilon_1=Q(e)W(e)+Q^*(d)W^*(d). \quad (6)$$

Of the two Q's, cross section $Q(e)$ is relatively the easier to measure by collecting the free electrons produced in a volume of gas in which the proton only makes one collision, and the results of various experimenters have been collected by Fite.[16] Recently Kuyatt and Jorgensen[17] (KJ), and Rudd and Jorgensen[18] (RJ) have measured $W(e)$ by determining the energies of the ejected electrons at various angles with an electrostatic analyzer and then integrating over energies and angles. KJ obtained relative values of $Q(e)$ and calculated absolute values by normalization to the results of Schwirzke[19]; RJ obtained an absolute value of $Q(e)$ at 100 keV. In Table VI we quote KJ's value of $Q(e)$ $W(e)$ at 50 keV, and RJ's value at 100 keV. RJ repeated the measurements of KJ at 100 keV and obtained a somewhat lower value than KJ, which may indicate that KJ's value at 50 keV is also somewhat high. Although Table VI shows values of $Q^*(d)W^*(d)/2\epsilon_1$, the numerators having been obtained by subtraction of $Q(e)W(e)$ from $2\epsilon_1$ as Eq. (6), very little reliability can be placed in the numbers $Q^*(d)W^*(d)$ thus obtained, since the quantities between which differences are being taken are each subject to errors of the order of 10% and the difference is about 10% of either quantity. The qualitative evidence is strong, however, that the energy expended in the production of free electrons in the gas is much greater (10×) than the energy expended in excitation and dissociation.

The calculations of Dalgarno and Griffing[20] (Table VI, Ref. f) for the passage of protons through atomic hydrogen gas separated the proton stopping power into four categories: (1) ionization; (2) excitation; (3) capture excitation; (4) capture momentum loss. Of these, (1) and (2) should contribute to ϵ_1, and in the table the ratio (2)/[(1)+(2)] as calculated by them is compared with $Q^*(d)W^*(d)/2\epsilon_1$ from experiment. The comparison indicates that the energy losses of protons in excitation and dissociation ($Q^*(d)W^*(d)$) of molecular hydrogen gas are even lower, relative to ionization ($Q(e)W(e)$) than their theoretical estimates for the atomic gas.

[14] A. Dalgarno, *Atomic and Molecular Processes*, edited by D. R. Bates (Academic Press Inc., New York, 1962), Chap. 15.
[15] W. Meckbach and S. K. Allison, Phys. Rev. **132**, 294 (1963). See Fig. 7.
[16] W. L. Fite, in *Atomic and Molecular Processes*, edited by D. R. Bates (Academic Press Inc., New York, 1962). Cf. Sec. 3.1.1, Chap. 12.
[17] C. E. Kuyatt and T. Jorgensen, Jr., Phys. Rev. **130**, 1444 (1963).
[18] M. E. Rudd and T. Jorgensen, Jr., Phys. Rev. **131**, 666 (1963).
[19] E. Schwirzke, Z. Physik **157**, 510 (1960).
[20] A. Dalgarno and G. W. Griffing, Proc. Roy. Soc. (London) **A232**, 423 (1955).

F. Partial Stopping Powers for H^0, He^+, He^0

Since exact solutions of the Schrödinger equation for nucleus plus single electron systems are known, the effectiveness of the screening of the nuclear charge at any radius may be computed. The result expressed as the net positive charge q within a sphere of radius r, is

$$q(r)=|e|[Z-1+(2r^2Z^2/a_0^2+2rZ/a_0+1)\times\exp(-2rZ/a_0)], \quad (7)$$

with $|e|$ the magnitude of the electronic charge, $Z|e|$ the nuclear charge, and $a_0=0.529\times10^{-8}$ cm. The corresponding electrostatic potential function is

$$V(r)=-|e|\left[\frac{Z-1}{r}+\left(\frac{1}{r}+\frac{Z}{a_0}\right)\exp\left(-\frac{2rZ}{a_0}\right)\right]. \quad (8)$$

For the configuration of two extra-nuclear electrons and a nucleus, approximations must be made, but probably a very elementary one, such as a screening correction, is sufficient. We have

$$V(r)=-|e|\left[\frac{Z-2}{r}+2\left(\frac{1}{r}+\frac{Z^*}{a_0}\right)\exp\left(-\frac{2rZ^*}{a_0}\right)\right], \quad (9)$$

with $Z=2$ and $Z^*=1.69$ for helium.[21]

For the calculation of stopping powers in atomic hydrogen gas the coordinate system used has its origin in the proton in the target atom. Vectors $\mathbf{r}_p$ and $\mathbf{r}_t$ locate the center of the oncoming screened charge projectile and of the electron in the target atom, respectively. Neglecting the interaction between the oncoming projectile and the proton in the target atom, the significant distance to insert in Eq. (9) is

$$r=|\mathbf{r}_p-\mathbf{r}_t|. \quad (10)$$

In standard treatments of stopping power[22] it is shown that the number of projectiles inelastically scattered per second from a beam of one per cm^2 per second, having experienced a momentum change $\hbar\kappa$, and at the same time excited the target atom from its normal state (0) to a state of total quantum number n is

$$I(\kappa)d\kappa=\frac{\mu^2}{2\pi\hbar^4k_p^2}\left|\int\int\psi_0\exp[i(k_{0n}\mathbf{n}_p'-k_p\mathbf{n}_0)\cdot\mathbf{r}_p]\times V(\mathbf{r}_p-\mathbf{r}_t)\psi_n^*d\mathbf{r}_pd\mathbf{r}_t\right|^2\kappa d\kappa. \quad (11)$$

The treatment is nonrelativistic, and in Born's approximation. μ is the reduced mass of projectile and target, in which the target is considered to be of electronic mass. k_p is $\mu v_p/\hbar$, with v_p the initial projectile velocity in the laboratory system. Ψ_0,Ψ_n^* are wave functions characterizing the initial and final states of the target atom. k_{0n} is λ^{-1} for the inelastically scattered projectile. $\mathbf{n}_0$, $\mathbf{n}_p'$ are unit vectors in the beam direction and in the direction of the scattered projectile, respectively.

Also we have

$$\kappa=|k_{0n}\mathbf{n}_p'-k_p\mathbf{n}_0|. \quad (12)$$

The integration is to be extended by conventional devices through the larger momentum changes corresponding to transitions to the continuum, which involve ionization of the target atom.

To illustrate the evaluation of Eq. (11) we will use the potential energy corresponding to the potential function of Eq. (8), with $Z=1$, i.e., the H^0 configuration. We first perform the integration over the coordinate $\mathbf{r}_p$ of the projectile. The integral is

$$e\int V(|\mathbf{r}_p-\mathbf{r}_t|)\exp(i\boldsymbol{\kappa}\cdot\mathbf{r}_p)dr_p=-e^2\int r^{-1}e^{i\kappa x_p}(1+\alpha_0 r)\exp(-2\alpha_0 r)d\mathbf{r}_p, \quad (13)$$

with $\kappa x_p=\boldsymbol{\kappa}\cdot\mathbf{r}_p$ and $\alpha_0=a_0^{-1}$. We remember that r involves r_p through Eq. (10). The evaluation of the integral of Eq. (13) requires some discussion, which is given in the standard treatments.[23] The result is

$$+4\pi e^2\left[\frac{a_0^2}{\kappa^2a_0^2+4}+\left(\frac{2a_0}{\kappa^2a_0^2+4}\right)^2\right]\exp(i\boldsymbol{\kappa}\cdot\mathbf{r}_t). \quad (14)$$

The stopping power of the target medium in ergs per atom per cm^2 is

$$-\frac{1}{N}\frac{dE}{dx}=\sum_n(E_0-E_n)\int_{\kappa_{min}}^{K}I(\kappa)d\kappa. \quad (15)$$

N is the number of target atoms per cm^3. E_0-E_n is the energy lost in the inelastic collision resulting in excitation to quantum state n.

The integration indicated in Eq. (15) is first performed between limits $\kappa_{\min}$ and κ_0, where $\kappa_0\sim\alpha_0$, and then from κ_0 to K where

$$\kappa_{\min}=8\pi^2\mu(E_n-E_0)/h^2K;\quad K=4\pi\mu v_p/h. \quad (16)$$

$K\hbar$ is the maximum linear momentum which can be transferred.

Since we are concerned with projectiles of atomic mass, μ is essentially the electronic mass. For the lower range of momentum transfers $\boldsymbol{\kappa}\cdot\mathbf{r}_t$ is small since $r_t\lesssim a_0$, and we make approximations in the exponential term of Eq. (14); in the upper range we make simplifications by means of the sum rule for oscillator strengths.[22] The resulting stopping power due to excitation and

[21] E. A. Hylleraas, Z. Physik **54**, 347 (1929).

[22] N. F. Mott and H. S. W. Massey, *The Theory of Atomic Collisions* (Oxford University Press, New York, 1949), 2nd ed. Cf. Eq. (8), p. 225.

[23] N. F. Mott and H. S. W. Massey, Ref. 22. H. A. Bethe, Ann. Physik **5**, 325 (1930).

TABLE VII. Nonrelativistic Born-approximation calculation of inelastic-collision energy losses through excitation and ionization of atomic hydrogen gas by various projectiles. Energy losses in (ergs per target atom per cm²) × $(mv^2/4\pi e^4)$.[a]

H^+ projectiles $\ln(2mv^2/1.105\,Rh)$	He^{++} projectiles $4\ln(2mv^2/1.105\,Rh)$	
H^0	He^0	He^+
$\frac{1}{2}\ln(4K^2a_0^2+16)$	$2\ln(K^2a_0^2+4Z^{*2})$	$\ln[2mv^2/1.105\ \mathrm{Rh}]$
$-2/(K^2a_0^2+4)$	$-8Z^{*2}/(K^2a_0^2+4Z^{*2})$	$+\frac{3}{2}\ln(K^2a_0^2+16)$
$+[2(K^2a_0^2+4)]^2$	$+16Z^{*4}/(K^2a_0^2+4Z^{*2})^2$	$-24/(K^2a_0^2+16)$
$+\frac{4}{3}[2/(K^2a_0^2+4)]^3$	$+(128/3)Z^{*6}/(K^2a_0^2+4Z^{*2})^3$	$+[8/(K^2a_0^2+16)]^2$
-1.303	-4.539	$+\frac{4}{3}[8/(K^2a_0^2+16)]^3$
		-3.075

[a] $m=9.11\times10^{-28}$ g, $e=4.80\times10^{-10}$ esu, v = projectile velocity in laboratory system in cm/sec, $Rh=2.178\times10^{-11}$ erg, $K=2mv/\hbar$ cm^{-1}, $a_0=0.529\times10^{-8}$ cm, $Z^*=1.69$, $h=6.62\times10^{-27}$ erg sec.

ionization of the target H^0 gas may be written

$$-\frac{1}{N}\frac{dE}{dx}=\frac{4\pi e^4}{\mu v_p^2}\times\left[S(K)-\frac{8\pi^2\mu R}{h}\sum\left(1-\frac{1}{n^2}\right)|X_n|^2S(\kappa_{\min})\right], \quad (17)$$

where $|X_n|^2=(h^2/8\pi^2\mu)[1/(E_n-E_0)]f_{0\to n}$, R is the Rydberg frequency, and $f_{0\to n}$ is the oscillator strength for the $0\to n$ transition, and

$$S(\kappa)=\ln 2(\kappa^2a_0^2+4)^{1/2}-\frac{2}{\kappa^2a_0^2+4}+\left(\frac{2}{\kappa^2a_0^2+4}\right)^2+\frac{4}{3}\left(\frac{2}{\kappa^2a_0^2+4}\right)^3. \quad (18)$$

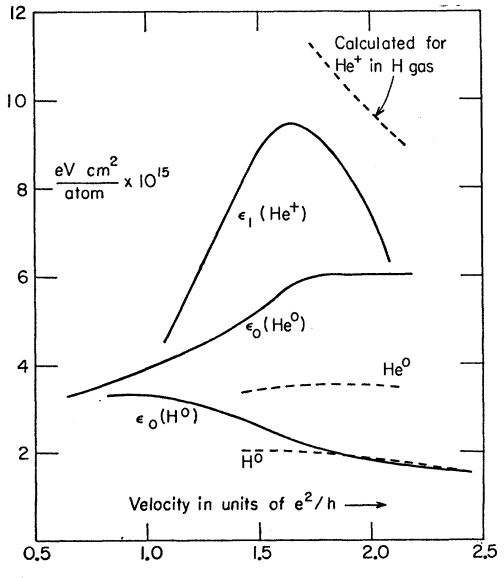

FIG. 7. The partial stopping powers of H_2 gas for H^0, He^0, and He^+ ions. Calculated curves are by Bethe's method but using screened charges. Theory and experiment are not strictly comparable; experimental ϵ_i values may include excitation of the projectile.

From Eq. (16), however, we find that since $\kappa_{\min}\ll\alpha_0$ the dependence of $S(\kappa_{\min})$ on (E_n-E_0) is very weak, actually, with negligible error, $S(\kappa_{\min})$ can be considered a constant for all terms of the sum and, using the sum rule

$$\frac{8\pi^2\mu R}{h}\sum\left(1-\frac{1}{n^2}\right)|X_n|^2=1, \quad (19)$$

we obtain

$$-\frac{1}{N}\frac{dE}{dx}=\frac{4\pi e^4}{\mu v_p^2}[S(K)-S(\kappa_{\min})], \quad (20)$$

in which

$$S(\kappa_{\min})=\ln 4-\tfrac{1}{2}+\tfrac{1}{4}+\tfrac{1}{6}=1.303. \quad (21)$$

The results of the H^0 and He^+ calculations are given in Table VII. This one electron problem has already been considered by Bates and Griffing,[24] with the same results. The He^+ problem has also been solved and published by Scott,[25] with a slightly different method of calculation.

Some numerical calculations from the formulas of Table VII are collected in Table VIII.

The stopping power of atomic hydrogen gas for H^0 atoms, computed as in Tables VII and VIII, and therefore neglecting the excitation and ionization of the projectile, is shown in Fig. 7 in comparison with the meas-

TABLE VIII. Stopping powers calculated by the nonrelativistic Born approximation, cf. Table VII. ϵ in units of (eV×cm²/atom) $\times10^{-15}$.

Velocity in units of $e^2/\hbar$	Hydrogen projectiles: Kinetic energy in keV	H^0 in H gas	H^+ in H gas	H^+ in H_2 gas	Helium projectiles: Kinetic energy in keV	He^0 in H gas	He^+ in H gas	He^{++} in H gas	He^{++} in H_2 gas
1.42	50	2.03	···	···	200	3.36	···	···	···
1.58	62.5	2.06	···	···	250	3.48	···	···	···
1.73	75	2.00	7.55	6.80	300	3.55	···	···	···
1.87	87.5	1.92	6.89	6.24	350	3.55	10.5	27.6	25.0
2.00	100	1.84	6.34	5.78	400	3.52	9.83	25.4	23.1
2.12	112.5	1.76	5.88	5.39	450	3.48	9.24	23.6	21.6
2.45	150	1.56	4.87	4.49	600	···	···	19.5	18.0

[24] D. R. Bates and G. Griffing, Proc. Phys. Soc. (London) **46**, 961 (1953).

[25] J. M. C. Scott, Proc. Cambridge Phil. Soc. **51**, 121 (1955).

ured $\epsilon_0(H^0)$. A more meaningful comparison, with calculations by Dalgarno and Griffing[20] was shown in a previous publication, but the comparison shown here indicates (as did the calculations) that excitation of the projectile without changing its charge is not a major source of stopping-power losses.

Detailed calculations such as those of Dalgarno and Griffing are not available for helium beams in hydrogen gas, and in comparison with our experimental $\epsilon_0(He^0)$ and $\epsilon_1(He^+)$ we can only show stopping powers calculated as in Tables VII and VIII, which are not strictly comparable to our ϵ_i values since they neglect excitation of the electronic structure of the projectile. The measured $\epsilon_1(He^+)$ lies below the calculated stopping power for He^+, as was the case for protons (see Fig. 6).

The greatest discrepancy is between the measured $\epsilon_0(He^0)$ values and the calculated stopping power for a He^0 projectile. The observed values of $\epsilon_0(He^0)$ are about 1.7 times the calculated neutral atom stopping power. The most obvious place to look for the source of the discrepancy is in collisions which excite the electrons in the He^0 structure without ionizing it, but the evidence from $\epsilon_0(H^0)$ indicates that not more than 10% of the stopping losses arise from such collisions, and the high partial atomic stopping power of He^0 awaits explanation.

ACKNOWLEDGMENT

We wish to thank John Erwood for construction of electrical equipment and general maintenance.

PHYSICAL REVIEW VOLUME 135, NUMBER 2A 20 JULY 1964

Fredholm Determinants Applied to Electron-Hydrogen Scattering*

GERALD L. NUTT
Lockheed Missiles and Space Company, Palo Alto, California
(Received 28 February 1964)

The properties of the Fredholm determinant for the electron-hydrogen atom system are discussed. These properties are used to derive formulas for the elastic-scattering phase shifts. S- and P-wave phase shifts are calculated for low energies and the results are compared with other recent calculations. Exchange effects are fully accounted for in the formalism, and a formula is given for the scattering amplitude when two exit channels are present.

I. INTRODUCTION

THE method of Fredholm determinants has been applied to low-energy meson-nucleon scattering by Baker.[1] Because this approach appears to have met with some success, it is interesting to ask whether Fredholm determinants can contribute anything to the theory of low-energy atomic scattering. Several desirable properties of this method suggest that they can.

One such property is the fact that unitarity is satisfied in all orders of approximation whereas the various approximations to the Born series do not satisfy the unitarity condition. Secondly, one obtains expressions for the phase shifts which, in the zero-energy region, are of the form prescribed by effective range theory. At higher energies, presumably the region where the Born series becomes valid, we obtain an expression which approaches the Born series.

In this paper we will treat the elastic scattering of electrons by atomic hydrogen in the energy region from near zero to about eight volts. No effective polarization potential will be included in the Hamiltonian, and the nucleus will be assumed to be static. The Hamiltonian is expressed in terms of the mass of the electrons and their charge as follows:

$$H=-\frac{1}{2m}\nabla_1^2-\frac{1}{2m}\nabla_2^2-\frac{e^2}{r_1}-\frac{e^2}{r_2}+\frac{e^2}{|\mathbf{r}_1-\mathbf{r}_2|}+E_R. \quad (1)$$

The constant E_R adjusts the energy levels of the system so that the eigenvalue of H is zero when the incoming particle has zero energy and the atom is in the ground state.

Although spin does not appear in the Hamiltonian, we will assume that the wave function for the system will include a description of the spin state. Thus, since we are dealing with two identical Fermi-Dirac particles, we will consider only those wave functions which are antisymmetric under simultaneous interchange of both the spatial as well as the spin coordinates.

We will divide the Hamiltonian into an unperturbed part, and an interaction term, denoted by H_0 and H_1, respectively:

$$H_0=-\frac{1}{2m}\nabla_1^2-\frac{1}{2m}\nabla_2^2-\frac{e^2}{r_2}+E_R, \quad (2)$$

$$H_1=-\frac{e^2}{r_1}+\frac{e^2}{|\mathbf{r}_1-\mathbf{r}_2|}. \quad (3)$$

* This work supported by the Lockheed Missiles and Space Company Independent Research Program and by the U. S. Air Force Weapons Laboratory, Air Force Systems Command under Contract AF 29(601)-6171.
[1] M. Baker, Ann. Phys. (N. Y.) 4, 271 (1958).